Table 2 continued

Rank	Gene symbol	Gene ID	Ratio	Gene name	Putative function
26	CXCL14	9547	2.45	Chemokine (C-X-C motif) ligand 14	A chemoattractant for monocytes and dendritic cells
27	ANXA1	301	2.30	Annexin A1	An annexin family protein with phospholipase A2 inhibitory activity
28	RCAN1	1827	2.29	Regulator of calcineurin 1	A negative regulator of calcineurin signaling
29	RPE65	6121	2.24	Retinal pigment epithelium-specific protein 65 kDa	A protein abundant in retinal pigment epithlium cells involved in the 11-cis retinol synthesis
30	STK17A	9263	2.22	Serine/threonine kinase 17a (apoptosis-inducing)	DAP kinase-related apoptosis-inducing protein kinase DRAK1
31	C4orf30	54876	2.22	Chromosome 4 open reading frame 30 C4orf30	Hypothetical protein LOC27146
32	CRYAB	1410	2.21	Crystallin, alpha B	A small HSP family protein
33	TMEM132B	114795	2.11	Transmembrane protein 132B	A transmembrane protein of unknown function
34	FZD1	8321	2.10	Frizzled homolog 1	A fizzled gene family protein that acts as a receptor for Wnt
35	ID2	3398	2.10	Inhibitor of DNA binding 2, dominant negative helix-loop-helix protein	A HLH protein that acts as a dominant negative regulator of bHLH family transcription factors
36	CDC42EP4	23580	2.09	CDC42 effector protein (Rho GTPase binding) 4	A CDC42-binding protein that interacts with Rho family GTPases
37	NCAN	1463	2.08	Neurocan	Chondroitin sulfate proteoglycan 3 involved in modulation of cell adhesion and migration
38	NAV2	89797	2.07	Neuron navigator 2	A helicase regulated by all-trans retinoic acid that plays a role in neuronal development
39	ENOX1	55068	2.06	Ecto-NOX disulfide-thiol exchanger 1	An enzymes with a hydroquinone (NADH) oxidase activity and a protein disulfide-thiol interchange activity
40	CLSTN2	64084	2.06	Calsyntenin 2	A postsynaptic membrane protein with Ca^{2+}-binding activity
41	NMB	4828	2.03	Neuromedin B	An amidated bombesin-like decapeptide
42	PCSK5	5125	2.02	Proprotein convertase subtilisin/kexin type 5	A member of the subtilisin-like proprotein convertase family
43	MAN1C1	57134	2.02	Mannosidase, alpha, class 1C, member 1	Alpha-1,2-mannosidase IC involved in N-glycan biosynthesis
44	GRAMD1C	54762	2.02	GRAM domain containing 1C	A protein with a GRAM motif of unknown function
45	VAT1	10493	2.01	Vesicle amine transport protein 1	An integral membrane protein of cholinergic synaptic vesicles involved in vesicular transport

Whole Human Genome Microarray (41,000 genes) was hybridized with Cy5-labeled cRNA of NPC incubated in the 10% FBS-containing culture medium and Cy3-labeled cRNA of NPC incubated in the serum-free culture medium. Upregulated genes in NPC by exposure to the serum are listed in order of greatness of the Cy5/Cy3 signal intensity ratio. The results of ID1, ID3, and GFAP (underlined) were validated by real-time RT-PCR analysis (see Fig. 3)

(CDC42EP4), neurocan (NCAN), neuron navigator 2 (NAV2), ecto-NOX disulfide-thiol exchanger 1 (ENOX1), calsyntenin 2 (CLSTN2), neuromedin B (NMB), proprotein convertase subtilisin/kexin type 5 (PCSK5), mannosidase alpha class 1C member 1 (MAN1C1), GRAM domain containing 1C (GRAMD1C), and vesicle amine transport protein 1 (VAT1).

It is worthy to note that three members of ID family genes, ID1, ID2, and ID3, were upregulated coordinately in the serum-treated NPC spheres. The ID family proteins that have an HLH domain but lack the DNA binding domain act as a dominant negative regulator of bHLH transcription factors (Ruzinova and Benezra 2003). Real-time RT-PCR and Western blot analysis validated marked upregulation of ID1, ID3, and GFAP in NPC following exposure to the serum (Fig. 3a–c, g, h). By immunocytochemistry, ID1 was located in the nucleus of GFAP-positive polygonal cells under the serum-containing culture condition

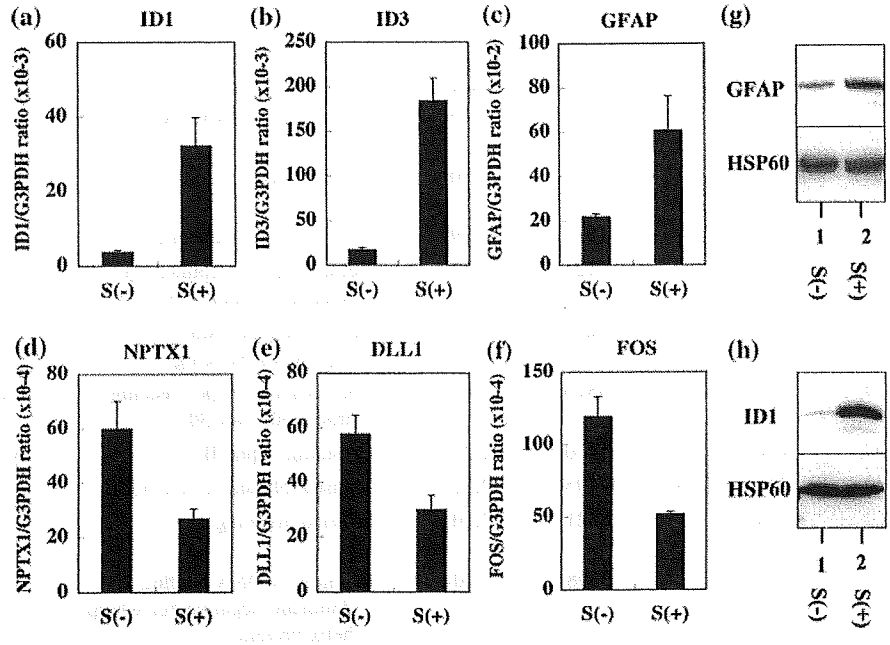

Fig. 3 Validation of microarray data by real-time RT-PCR and western blot analysis. Human NPC spheres were incubated for 72 h in the NPC medium with (S+) or without (S−) inclusion of 10% FBS, and then total cellular RNA or protein extract was processed for real-time RT-PCR and western blot analysis. **a–f** Real-time RT-PCR. The levels of target genes were standardized against the levels of the G3PDH gene. **a** ID1, **b** ID3, **c** GFAP, **d** NPTX1, **e** DLL1, and **f** FOS. **g**, **h** Western blot. The blots were reprobed with anti-HSP60 antibody to serve HSP60 for an internal control. **g** GFAP and **h** ID1

(Fig. 2c). Because GFAP is a defining marker of astrocytes, the results of microarray, RT-PCR, and Western blot verified that the serum promotes astrocyte differentiation of NPC.

Downregulated Genes in Human NPC Following Exposure to the Serum

Exposure of NPC to the serum reduced the levels of expression of 23 genes (Table 3). They include neuronal pentraxin I (NPTX1), cerebellin 4 (CBLN4), delta-like 1 (DLL1), cellular oncogene c-fos (FOS), SPARC related modular calcium binding 1 (SMOC1), matrilin 2 (MATN2), platelet-derived growth factor receptor alpha (PDGFRA), ryanodine receptor 3 (RYR3), transferrin receptor (TFRC), pleckstrin homology domain containing family H member 2 (PLEKHH2), delta-like 3 (DLL3), SRY-box 4 (SOX4), myosin VC (MYO5C), protocadherin 8 (PCDH8), ankyrin repeat domain 10 (ANKRD10), glutamate receptor ionotropic kainate 1 (GRIK1), chondroitin sulfate proteoglycan 4 (CSPG4), cystatin C (CST3), secreted frizzled-related protein 1 (SERP1), ryanodine receptor 1 (RYR1), growth arrest-specific 1 (GAS1), cystatin D (CST5), and hairy and enhancer of split 5 (HES5).

It is worthy to note that the list of downregulated genes included two Notch ligand Delta family members, DLL1 and DLL3, and a Notch effector HES5. It is well known that Notch signaling regulates cell fate specification and multipotency of NSC and NPC (Yoshimatsu et al. 2006). Real-time RT-PCR analysis validated substantial downregulation of NPTX1, DLL1, and FOS in the serum-treated NPC (Fig. 2d–f).

Functional Annotation of the Serum-Responsive Genes in Human NPC

To investigate the functional annotation of the serum-responsive genes in human NPC identified by microarray analysis, the list of Entrez Gene IDs of 45 serum-upregulated genes and 23 serum-downregulated genes was uploaded onto the DAVID database. Top 5 most significant biological processes relevant to the panel of these genes consisted of developmental process (GO:0032502; 32 genes; *P*-value = 2.0E-9), anatomical structure development (GO:0048856; 26 genes; *P*-value = 4.2E-9), multicellular organismal development (GO:0007275; 26 genes; *P*-value = 2.5E-8), system development (GO:0048 731; 20 genes; *P*-value = 2.2E–6), and anatomical structure morphogenesis (GO:0009653; 16 genes; *P*-value = 3.2E–6). The genes involved in the category GO:0032502 include the serum-upregulated genes such as IDI, ID2, ID3, CTGF, TGFA, METRN, KLF9, SULF1, AGT, GADD45B, ANXA1, RCAN1, RPE65, STK17A, CRYAB, FZD1, CDC42EP4, and VAT1, and the serum-downregulated genes such as DLL1, DLL3, HES5, NPTX1, FOS, PDGFRA, RYR1, RYR3, SOX4, PCDH8, GRIK1, CSPG4, SERP1, and GAS1. Thus, the genes whose expression levels were drastically changed in NPC by exposure to the serum are clustered in GO functional categories termed "development."

ID1 Acts as a Negative Regulator of DLL1 Expression

Since the serum-induced astrocyte differentiation of human NPC was followed by remarkable upregulation of ID1, ID2,

Table 3 Downregulated genes in human neuronal progenitor cells (NPC) following exposure to the serum

Rank	Gene symbol	Gene ID	Ratio	Gene name	Putative function
1	NPTX1	4884	0.26	Neuronal pentraxin I	A member of the neuronal pentraxin gene family involved in synaptic plasticity
2	CBLN4	140689	0.36	Cerebellin 4 precursor	A glycoprotein with sequence similarity to precerebellin
3	DLL1	28514	0.38	Delta-like 1	A Notch ligand involved in intercellular communication
4	FOS	2353	0.39	v-fos FBJ murine osteosarcoma viral oncogene homolog	A component of the AP-1 transcription factor complex
5	SMOC1	64093	0.41	SPARC related modular calcium binding 1	A secreted modular calcium-binding glycoprotein in basement membrane
6	MATN2	4147	0.43	Matrilin 2	A filament-forming protein widely distributed in extracellular matrices
7	PDGFRA	5156	0.44	Platelet-derived growth factor receptor, alpha polypeptide	A PDGF receptor component
8	RYR3	6263	0.44	Ryanodine receptor 3	An intracellular calcium release channel
9	TFRC	7037	0.44	Transferrin receptor (p90, CD71)	A gatekeeper for regulating iron
10	PLEKHH2	130271	0.45	Pleckstrin homology domain containing, family H (with MyTH4 domain) member 2	A cytoskeletal protein involved in cell growth
11	DLL3	10683	0.46	Delta-like 3	A Notch ligand involved in intercellular communication
12	SOX4	6659	0.46	SRY (sex determining region Y)-box 4	A member of the SOX family transcription factor involved in the regulation of embryonic development
13	MYO5C	55930	0.46	Myosin VC	A myosin superfamily protein involved in transferrin trafficking
14	PCDH8	5100	0.47	Protocadherin 8	A member of the protocadherin gene family involved in cell adhesion
15	ANKRD10	55608	0.48	Ankyrin repeat domain 10	A protein with ankyrin repeats of unknown function
16	GRIK1	2897	0.48	Glutamate receptor, ionotropic, kainate 1	Ionotropic glutamate receptor subunit GluR5
17	CSPG4	1464	0.48	Chondroitin sulfate proteoglycan 4 (melanoma-associated; NG2)	Chondroitin sulfate proteoglycan that plays a role in stabilizing cell-substratum interaction
18	CST3	1471	0.48	Cystatin C (amyloid angiopathy and cerebral hemorrhage)	An extracellular inhibitor of cycteine proteases
19	SFRP1	6422	0.49	Secreted frizzled-related protein 1	A soluble inhibitor for Wnt signaling
20	RYR1	6261	0.49	Ryanodine receptor 1 (skeletal)	A calcium release channel of the sarcoplasmic reticulum
21	GAS1	2619	0.49	Growth arrest-specific 1	A GPI-anchored protein expressed at growth arrest
22	CST5	1473	0.50	Cystatin D	An extracellular inhibitor of cysteine proteases
23	HES5	388585	0.50	Hairy and Enhancer of split 5 (Drosophila)	bHLH transcription factor downstream of Notch signaling

Whole Human Genome Microarray (41,000 genes) was hybridized with Cy5-labeled cRNA of NPC incubated in the 10% FBS-containing culture medium and Cy3-labeled cRNA of NPC incubated in the serum-free culture medium. Downregulated genes in NPC by exposure to the serum are listed in order of smallness of the Cy5/Cy3 signal intensity ratio. The results of NPTX1, DLL1, and FOS (underlined) were validated by real-time RT-PCR analysis (see Fig. 3)

and ID3, and concomitant downregulation of DLL1 and DLL3, we studied the possible inverse relationship between ID family and Delta family genes with respect to regulation of gene expression. First, by real-time RT-PCR, we determined the levels of ID1 and DLL1 expression in various human neural and non-neural cell lines. The levels of ID1 expression are high but those of DLL1 are very low in HMO6, and HeLa, HepG2, U-373MG, and SK-N-SH, whereas the levels of DLL1 expression are high but those of ID1 are much lower in NTera2 N and IMR-32 (Fig. 4a, b).

Next, we investigated the molecular network of ID1, ID2, ID3, DLL1, and DLL3 by KeyMolnet, a bioinformatics tool for analyzing molecular interaction on the curated knowledge database. The "N-points to N-points" search of KeyMolnet illustrated the shortest route connecting the start point molecules of ID1, ID2, and ID3 and the end point molecules DLL1 and DLL3 (Fig. 5). The pathway based on the molecules showed a significant relationship with canonical pathways of KeyMolnet library, such as transcriptional regulation by SMAD (P-value = 6.6E–12), transcriptional regulation by CREB (P-value = 7.8E–11), and Notch signaling pathway (P-value = 9.7E–9). Although no direct interaction was identified between ID family and Delta family genes,

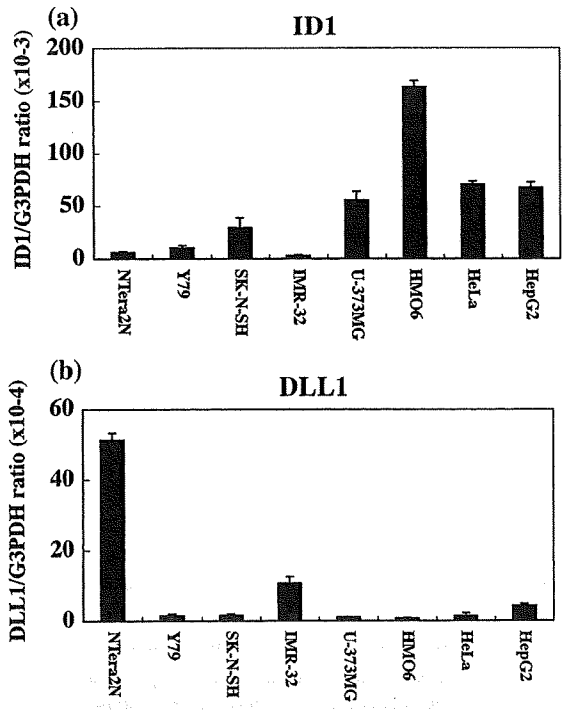

Fig. 4 ID1 and DLL1 expression in various human cell lines. Total RNA of human cell lines, such as NTera2 teratocarcinoma, Y79 retinoblastoma, SK-N-SH neuroblastoma, IMR-32 neuroblastoma, U-373MG astrocytoma, HMO6 microglia, HeLa cervical carcinoma, and HepG2 hepatoblastoma was processed for real-time RT-PCR analysis. The levels of target genes were standardized against the levels of the G3PDH gene. **a** ID1 and **b** DLL1

KeyMolnet indicated two proneural bHLH genes, such as human achaete-scute homolog 1 (HASH1, also known as MASH1 or ASCL) and neurogenin 3 (NGN3, NEUROG3), both of which have an indirect connection with ID1, ID2 and ID3 via HES1, and a T-box gene family member TBX18 as principal regulators of DLL1 expression (Fig. 5). Because microarray analysis indicated that MASH1 is expressed in NPC spheres at much higher levels than NGN3 (data not shown), we confined our attention to a role of MASH1 in the counterbalance between ID and Delta family genes in regulation of gene expression.

Next, we studied the molecular interaction between ID1 and MASH1. By immunoprecipitation analysis of recombinant ID1 and MASH1 proteins coexpressed in HEK293 cells, we identified a direct interaction between ID1 and MASH1 (Fig. 6a, b, lane 2). Then, we cloned two non-overlapping sequences of the human DLL1 promoter containing several E-box sequences, consisting of the region #1 spanning −1,253 and −254 or the region #2 spanning −2,946 and −1,786, in the luciferase reporter vector. Dual luciferase assay indicated that both DLL1 promoter sequences were activated by the expression of MASH1, but this activation was suppressed by the coexpression of ID1 (Fig. 6c, d).

BMP4 Upregulates ID1 and GFAP Expression in Human NPC

Previous studies showed that the serum contains substantial amounts of BMP4 (Kodaira et al. 2006). Because the serum-induced astrocyte differentiation of human NPC was followed by robust upregulation of ID1, we studied the direct effect of BMP4 on expression of ID1 and GFAP in human NPC. When incubated under the serum-free NPC medium, a 72 h-treatment of NPC with 50 ng/ml BMP4 greatly elevated the levels of ID1 and GFAP mRNA expression, suggesting that BMP4 serves as a candidate for astrocyte-inducing factors included in the serum (Fig. 7a, b).

Discussion

We studied the effect of the serum on gene expression profile of cultured human NPC to identify the gene signature of the astrocyte differentiation of human NPC. Following exposure to the serum, human NPC spheres rapidly attached on the plastic surface, and subsequently, adherent cells were differentiated into astrocytes, accompanied by upregulation of GFAP expression, consistent with the previous studies on the rodent NSC and NPC (Chiang et al. 1996; Brunet et al. 2004). The serum elevated the levels of expression of 45 genes in human NPC, including three ID family members ID1, ID2, and ID3, all of which are direct target genes regulated by bone morphogenetic proteins (BMP) (Hollnagel et al. 1999). In contrast, the serum reduced the expression of 23 genes in human NPC, including three Delta-Notch signaling components DLL1, DLL3, and HES5. ID proteins act as a dominant negative regulator of bHLH transcription factors by binding to the ubiquitously expressed bHLH E proteins, such as E2A gene products E12 and E47, or by binding to the cell lineage-restricted bHLH transcription factors (Langlands et al. 1997; Nakashima et al. 2001). By *in silico* molecular network analysis of ID1, ID2, ID3, DLL1, and DLL3 on KeyMolnet, we identified MASH1 as one of important regulators of DLL1 expression. Furthermore, by coimmunoprecipitation analysis, we identified ID1 as a direct binding partner of MASH1. By luciferase assay, we found that activation of DLL1 promoter by MASH1 was counteracted by ID1. Finally, we found that BMP4 elevated the levels of ID1 and GFAP expression in NPC under the serum-free culture conditions. Because the serum contains substantial amounts of BMP4 (Kodaira et al. 2006), our observations raise the possible scenario that the serum factor(s), most probably BMP4, induces astrocyte differentiation by upregulating the expression of ID family genes that repress the proneural bHLH protein-mediated Delta expression in human NPC (Fig. 8).

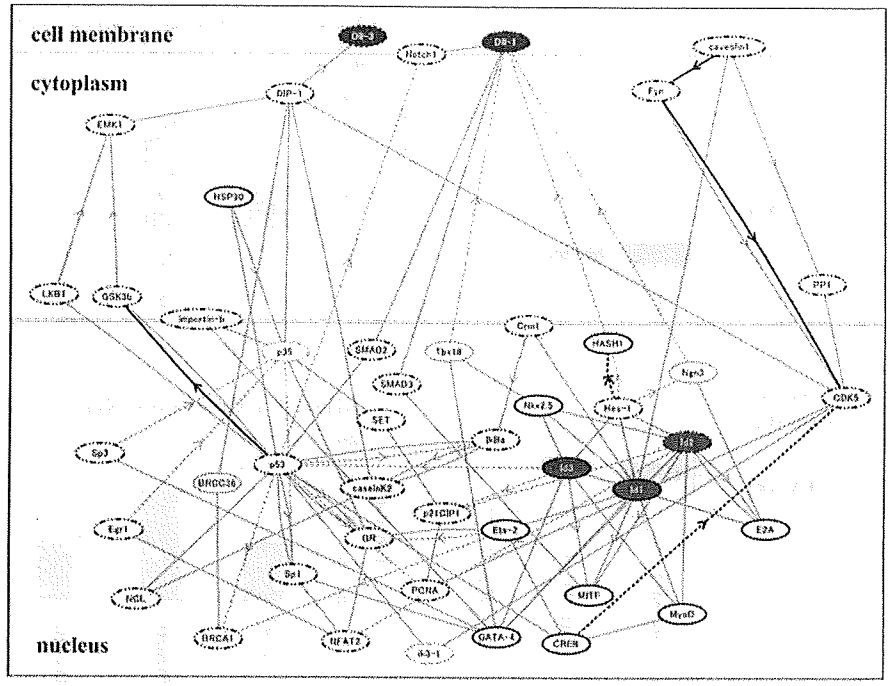

Fig. 5 Molecular network analysis of ID1, ID2, ID3, DLL1, and DLL3. KeyMolnet, a bioinformatics tool for analyzing molecular interaction on the curated knowledge database, identified the shortest route connecting the start point molecules of ID1, ID2, and ID3 (red) and the end point molecules DLL1 and DLL3 (blue). The pathway based on the molecules showed a significant relationship with transcriptional regulation by SMAD or CREB and Notch signaling pathway. The molecular network indicated HASH1 (MASH1), neurogenin 3 (NGN3), and TBX18 as principal regulators of DLL1 expression. The molecular relation is shown by solid line with arrow (direct binding or activation), solid line without arrow (complex formation), and dash line with arrow (transcriptional activation), and dash line with arrow and stop (transcriptional repression). Thick lines indicate the core contents, while thin lines indicate the secondary contents of KeyMolnet

The Serum-Induced Astrocyte Differentiation of Human NPC is Characterized by a Counteraction of ID Family Genes on Delta Family Genes

We proposed the hypothesis that ID genes act as a key positive regulator of the serum-induced astrocyte differentiation of human NPC. The following previous observations support this view. The expression of four ID members is transiently elevated in immortalized mouse astrocyte precursor cells during astrocyte differentiation (Andres-Barquin et al. 1997). ID gene expression is rapidly induced in cultured rat astrocytes following stimulation with the serum (Tzeng and de Vellis 1997). Treatment of rodent NPC with BMP4 induces the expression of four ID genes, followed by induction of astrocyte differentiation, while the complex formation of ID4 or ID2 with bHLH proteins OLIG1 and OLIG2 blocks oligodendrocyte lineage commitment (Samanta and Kessler 2004).

ID proteins also act as a negative regulator of neuronal differentiation by preventing premature exit of neuroblasts from the cell cycle (Lyden et al. 1999). Retroviral vector-mediated overexpression of ID1 in the mouse brain in vivo inhibits neurogenesis but promotes astrocytogenesis (Cai et al. 2000). BMP2 induces the expression of ID1 and ID3, which inhibit the transcriptional activity of MASH1 and E47 complex on an E-box-containing promoter, suggesting that ID protein-mediated antagonism of proneural bHLH transcription factors plays a role in inhibition of neuronal differentiation (Nakashima et al. 2001). Combinatorial actions of proneural bHLH and inhibitory HLH factors regulate the timing of differentiation of NPC (Kageyama et al. 2005). ID1 binds not only to E proteins but also to myogenic bHLH transcription factors MYOD and MYF5 with high affinity (Langlands et al. 1997). We found that ID1 is a direct binding partner of neurogenic bHLH transcription factor MASH1. MASH1 deficient mice showed a severe loss of NPC in the subventricular zone of the medial ganglionic eminence, and MASH1, expressed in NPC, regulates neuronal differentiation by inducing the expression of Notch ligands DLL1 and DLL3, resulting in activation of Notch signaling in adjacent cells (Casarosa et al. 1999; Ito et al. 2000). Importantly, Mash1 directly activates the promoter of DLL1 gene (Castro et al. 2006). The activation of Delta-Notch signaling plays a key role in maintenance of NPC in the undifferentiated state (Yoshimatsu et al. 2006).

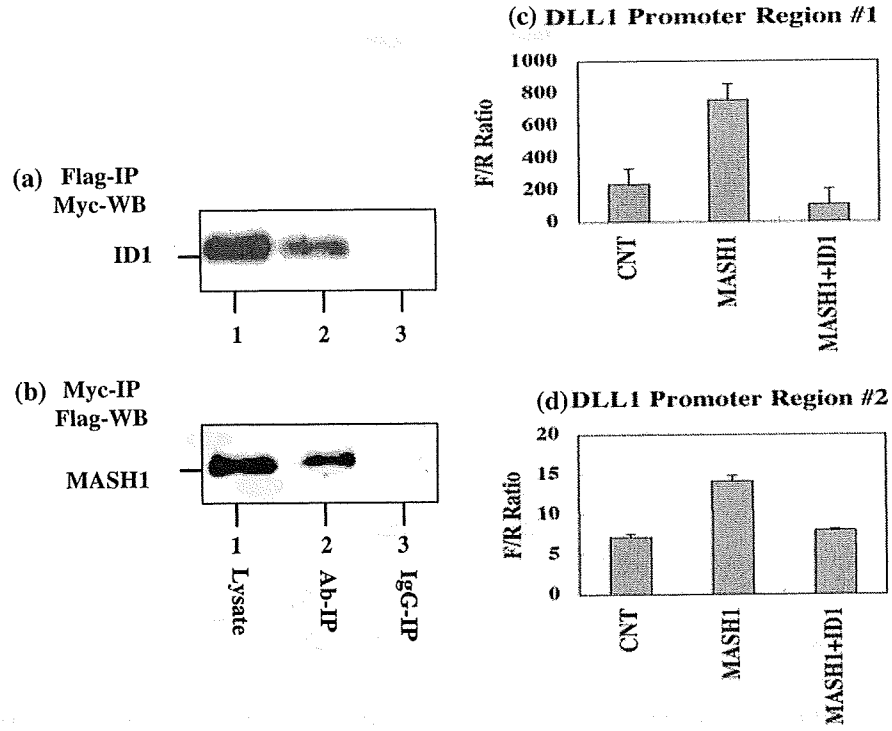

Fig. 6 Activation of the DLL1 promoter by MASH1 was counteracted by ID1. **a**, **b** Coimmunoprecipitation analysis. Recombinant MASH1 protein tagged with Flag and ID1 protein tagged with Myc were coexpressed in HEK293 cells. Immunoprecipitation (IP) followed by Western blotting (WB) was performed by using the antibodies against Flag and Myc. The lanes (1–3) represent (1) input control of cell lysate, (2) IP with anti-Flag or anti-Myc antibody, and (3) IP with normal mouse or rabbit IgG. **c**, **d** Dual luciferase assay. Two non-overlapping regions of the human DLL1 promoter, consisting of the region #1 spanning −1,253 and −254 or the region #2 spanning −2,946 and −1,786, were cloned into the Firefly luciferase reporter vector. It was co-transfected with the Renilla luciferase reporter vector (an internal control) in HEK293 cells, which were introduced with none (CNT), MASH1, or both MASH1 and ID1 expression vectors at 36 h before transfection of the luciferase reporter vectors. At 16 h after transfection of the luciferase reporter vectors, cell lysate was processed for dual luciferase assay. The ratio of Firefly (F)/Renilla (R) luminescence (RLU) is indicated

Fig. 7 BMP4 upregulates ID1 and GFAP expression in human NPC. Human NPC were incubated for 72 h in the NPC medium with (+) or without (−) inclusion of 50 ng/ml recombinant human BMP4, and then total cellular RNA was processed for real-time RT-PCR analysis. The levels of target genes were standardized against the levels of the G3PDH gene. **a** ID1 and **b** GFAP

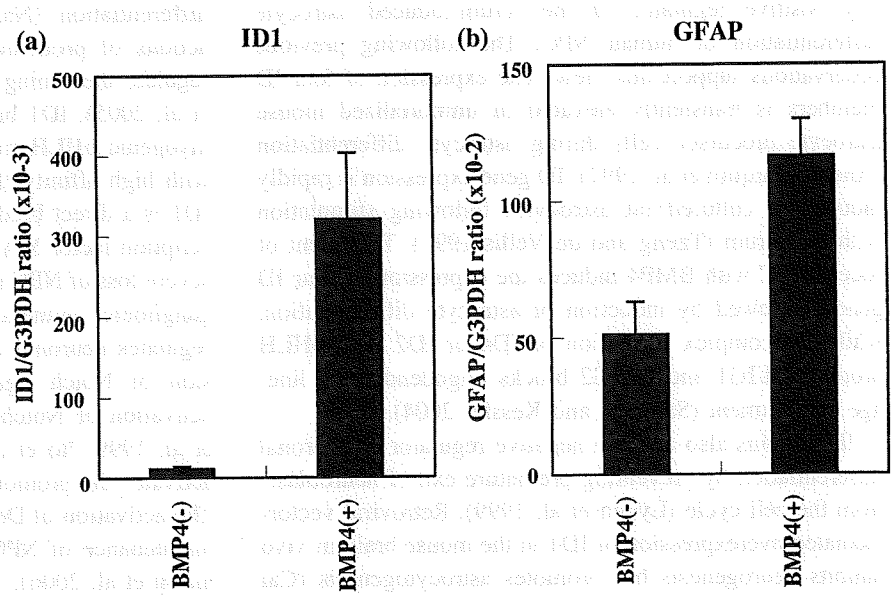

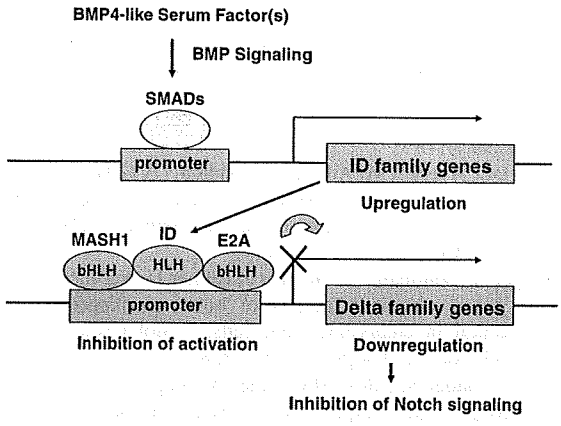

Fig. 8 The serum-induced astrocyte differentiation of human NPC is characterized by a counteraction between ID and Delta family genes. The present observations raise the possible scenario that the serum factor(s), most probably BMP4, induces astrocyte differentiation by upregulating the expression of ID family genes that repress the proneural bHLH protein, probably MASH1-mediated Delta expression in human NPC

The Serum-Induced Astrocyte Differentiation of Human NPC is Accompanied by Upregulation of Astrocyte Function-Related Genes

The serum-induced astrocyte differentiation of human NPC elevated the expression of astrocyte function-related genes (Table 2). Astrocytes express angiotensinogen (AGT) that plays a role in maintenance of the blood–brain barrier (BBB) function (Kakinuma et al. 1998). Astrocytes synthesize cathepsin H (CTSH) that acts as a metabolizing enzyme for neuropeptides and bradykinin (Brguljan et al. 2003). Human astrocytes in culture express complement factor I (CFI) essential for regulating the complement cascade (Gordon et al. 1992). Neuronal and glial progenitor cells secrete meterorin (METRN) that stimulates astrocyte differentiation in culture (Nishino et al. 2004). Calcineurin-dependent calcium signals induce the expression of regulator of calcineurin 1 (RCAN1) in astrocytes, an endogenous calcineurin inhibitor (Canellada et al. 2008).

Reactive astrocytes express connective tissue growth factor (CTGF), a TGF-β1 downstream mediator, involved in glial scar formation (Schwab et al. 2000). Reactive astrocytes express EGFR in response to various insults, and produce transforming growth factor alpha (TGFA) that triggers astrogliosis (Rabchevsky et al. 1998). Reactive astrocytes in Alzheimer disease brains express collectin sub-family member 12 (COLEC12), a member of the scavenger receptor family, which plays a role in amyloid-β clearance (Nakamura et al. 2006). Reactive astrocytes in multiple sclerosis brains express annexin A1 (ANXA1), a calcium-dependent phospholipid-binding protein that acts as an anti-inflammatory mediator (Probst-Cousin et al. 2002). At the site of spinal cord injury, reactive astrocytes produce neurocan (NCAN), a member of the CSPG family, which inhibits axonal regeneration (Jones et al. 2003).

Several serum-responsive genes have implications in astrocyte oncogenesis. FGF binding protein 2 (FGFBP2) is overexpressed in astrocytic tumors (Yamanaka et al. 2006). The expression of regulator of G-protein signaling 4 (RGS4), a negative regulator of G-protein signaling, is elevated in astrocytic tumor cells with a highly migratory capacity (Tatenhorst et al. 2004). Both chitinase 3-like 2 (CHI3L2) and neuromedin B (NMB) are identified as an astrocytoma-associated gene by serial analysis of gene expression (SAGE) profiles (Boon et al. 2004).

The Serum-Induced Astrocyte Differentiation of Human NPC is Accompanied by Downregulation of NPC and Neuronal Function-Related Genes

The serum-induced astrocyte differentiation of human NPC reduced the expression of NPC and neuronal function-related genes (Table 3). Neuronal pentaraxin I (NPTX1) plays a key role in activity-dependent plasticity of excitatory synapses (Xu et al. 2003). Protocadherin 8 (PCDH8) is a neuronal activity-regulated cadherin involved in long-term potentiation in the hippocampus (Yamagata et al. 1999). Spinal cord motor neurons express the ionotropic kainite receptor subunit GRIK1 (GluR5) (Eubanks et al. 1993). Ryanodine receptors RyR1, RyR2, and RyR3 are intracellular calcium release channels expressed in subpopulations of neurons in the human CNS (Martin et al. 1998).

NPC expressing the PDGF α-receptor (PDGFRA) proliferate in response to PDGF-AA associated with induction of c-fos (FOS) expression (Erlandsson et al. 2001). NPC express the transferrin receptor (TFRC, CD71) (Sergent-Tanguy et al. 2006), while oligodendrocyte progenitor cells express NG2 (CSPG4), an integral membrane chondroitin sulfate proteoglycan (Chang et al. 2000). NSC and NPC secrete cystatin C (CST3) into the culture medium, serving as a survival factor (Taupin et al. 2000). Growth arrest-specific 1 (GAS1) induced by Wnt signaling is required for proliferation of progenitors of the cerebellar granule cells and Bergmann glia (Liu et al. 2001). The HMG-box transcription factor Sox4, expressed in neuronal as well as glial progenitors, is downregulated in terminally differentiated neurons or glia (Hoser et al. 2007). Importantly, a recent study by microarray analysis showed that fetal human NPC express PDGFRA, CSPG4, DLL3, GAS1, and SOX4 (Maisel et al. 2007), all of which are downregulated in the serum-treated NPC in the present study.

In summary, we identified 45 serum-upregulated and 23 serum-downregulated genes in human NPC in culture by analysis with a whole human genome-scale microarray. The serum-induced astrocyte differentiation of human NPC

is characterized by a counteraction of ID family genes on Delta family genes.

Acknowledgments This work was supported by a research Grant to J-IS from the High-Tech Research Center Project, the Ministry of Education, Culture, Sports, Science and Technology (MEXT), Japan (S0801043).

References

Andres-Barquin PJ, Hernandez MC, Hayes TE, McKay RD, Israel MA (1997) Id genes encoding inhibitors of transcription are expressed during in vitro astrocyte differentiation and in cell lines derived from astrocytic tumors. Cancer Res 57:215–220

Boon K, Edwards JB, Eberhart CG, Riggins GJ (2004) Identification of astrocytoma associated genes including cell surface markers. BMC Cancer 4:39. doi:10.1186/1471-2407-4-39

Brguljan PM, Turk V, Nina C, Brzin J, Krizaj I, Popovic T (2003) Human brain cathepsin H as a neuropeptide and bradykinin metabolizing enzyme. Peptides 24:1977–1984. doi:10.1016/j.peptides.2003.09.018

Brunet JF, Grollimund L, Chatton JY, Lengacher S, Magistretti PJ, Villemure JG, Pellerin L (2004) Early acquisition of typical metabolic features upon differentiation of mouse neural stem cells into astrocytes. Glia 46:8–17. doi:10.1002/glia.10348

Cai L, Morrow EM, Cepko CL (2000) Misexpression of basic helix-loop-helix genes in the murine cerebral cortex affects cell fate choices and neuronal survival. Development 127:3021–3030

Cai Y, Wu P, Ozen M, Yu Y, Wang J, Ittmann M, Liu M (2006) Gene expression profiling and analysis of signaling pathways involved in priming and differentiation of human neural stem cells. Neuroscience 138:133–148. doi:10.1016/j.neuroscience.2005.11.041

Canellada A, Ramirez BG, Minami T, Redondo JM, Cano E (2008) Calcium/calcineurin signaling in primary cortical astrocyte cultures: Rcan1-4 and cyclooxygenase-2 as NFAT target genes. Glia 56:709–722. doi:10.1002/glia.20647

Carpenter MK, Cui X, Hu ZY, Jackson J, Sherman S, Seiger A, Wahlberg LU (1999) In vitro expansion of a multipotent population of human neural progenitor cells. Exp Neurol 158:265–278. doi:10.1006/exnr.1999.7098

Casarosa S, Fode C, Guillemot F (1999) Mash1 regulates neurogenesis in the ventral telencephalon. Development 126:525–534

Castro DS, Skowronska-Krawczyk D, Armant O, Donaldson IJ, Parras C, Hunt C, Critchley JA, Nguyen L, Gossler A, Göttgens B, Matter JM, Guillemot F (2006) Proneural bHLH and Brn proteins coregulate a neurogenic program through cooperative binding to a conserved DNA motif. Dev Cell 11:831–844. doi:10.1016/j.devcel.2006.10.006

Chang A, Nishiyama A, Peterson J, Prineas J, Trapp BD (2000) NG2-positive oligodendrocyte progenitor cells in adult human brain and multiple sclerosis lesions. J Neurosci 20:6404–6412

Chiang YH, Silani V, Zhou FC (1996) Morphological differentiation of astroglial progenitor cells from EGF-responsive neurospheres in response to fetal calf serum, basic fibroblast growth factor, and retinol. Cell Transplant 5:179–189. doi:10.1016/0963-6897(95)02043-8

Dennis G Jr, Sherman BT, Hosack DA, Yang J, Gao W, Lane HC, Lempicki RA (2003) DAVID: database for annotation, visualization, and integrated discovery. Genome Biol 4:R60. doi:10.1186/gb-2003-4-9-r60

Erlandsson A, Enarsson M, Forsberg-Nilsson K (2001) Immature neurons from CNS stem cells proliferate in response to platelet-derived growth factor. J Neurosci 21:3483–3491

Eubanks JH, Puranam RS, Kleckner NW, Bettler B, Heinemann SF, McNamara JO (1993) The gene encoding the glutamate receptor subunit GluR5 is located on human chromosome 21q21.1–22.1 in the vicinity of the gene for familial amyotrophic lateral sclerosis. Proc Natl Acad Sci USA 90:178–182. doi:10.1073/pnas.90.1.178

Gordon DL, Avery VM, Adrian DL, Sadlon TA (1992) Detection of complement protein mRNA in human astrocytes by the polymerase chain reaction. J Neurosci Methods 45:191–197. doi:10.1016/0165-0270(92)90076-P

Hollnagel A, Oehlmann V, Heymer J, Rüther U, Nordheim A (1999) Id genes are direct targets of bone morphogenetic protein induction in embryonic stem cells. J Biol Chem 274:19838–19845. doi:10.1074/jbc.274.28.19838

Hoser M, Baader SL, Bösl MR, Ihmer A, Wegner M, Sock E (2007) Prolonged glial expression of Sox4 in the CNS leads to architectural cerebellar defects and ataxia. J Neurosci 27:5495–5505. doi:10.1523/JNEUROSCI.1384-07.2007

Ishii K, Nakamura M, Dai H, Finn TP, Okano H, Toyama Y, Bregman BS (2006) Neutralization of ciliary neurotrophic factor reduces astrocyte production from transplanted neural stem cells and promotes regeneration of corticospinal tract fibers in spinal cord injury. J Neurosci Res 84:1669–1681. doi:10.1002/jnr.21079

Ito T, Udaka N, Yazawa T, Okudela K, Hayashi H, Sudo T, Guillemot F, Kageyama R, Kitamura H (2000) Basic helix-loop-helix transcription factors regulate the neuroendocrine differentiation of fetal mouse pulmonary epithelium. Development 127:3913–3921

Jones LL, Margolis RU, Tuszynski MH (2003) The chondroitin sulfate proteoglycans neurocan, brevican, phosphacan, and versican are differentially regulated following spinal cord injury. Exp Neurol 182:399–411. doi:10.1016/S0014-4886(03)00087-6

Kageyama R, Ohtsuka T, Hatakeyama J, Ohsawa R (2005) Roles of bHLH genes in neural stem cell differentiation. Exp Cell Res 306:343–348. doi:10.1016/j.yexcr.2005.03.015

Kakinuma Y, Hama H, Sugiyama F, Yagami K, Goto K, Murakami K, Fukamizu A (1998) Impaired blood-brain barrier function in angiotensinogen-deficient mice. Nat Med 4:1078–1080. doi:10.1038/2070

Kodaira K, Imada M, Goto M, Tomoyasu A, Fukuda T, Kamijo R, Suda T, Higashio K, Katagiri T (2006) Purification and identification of a BMP-like factor from bovine serum. Biochem Biophys Res Commun 345:1224–1231. doi:10.1016/j.bbrc.2006.05.045

Langlands K, Yin X, Anand G, Prochownik EV (1997) Differential interactions of Id proteins with basic-helix-loop-helix transcription factors. J Biol Chem 272:19785–19793. doi:10.1074/jbc.272.32.19785

Liu Y, May NR, Fan CM (2001) Growth arrest specific gene 1 is a positive growth regulator for the cerebellum. Dev Biol 236:30–45. doi:10.1006/dbio.2000.0146

Lyden D, Young AZ, Zagzag D, Yan W, Gerald W, O'Reilly R, Bader BL, Hynes RO, Zhuang Y, Manova K, Benezra R (1999) Id1 and Id3 are required for neurogenesis, angiogenesis and vascularization of tumour xenografts. Nature 401:670–677. doi:10.1038/44334

Maisel M, Herr A, Milosevic J, Hermann A, Habisch HJ, Schwarz S, Kirsch M, Antoniadis G, Brenner R, Hallmeyer-Elgner S, Lerche H, Schwarz J, Storch A (2007) Transcription profiling of adult and fetal human neuroprogenitors identifies divergent paths to maintain the neuroprogenitor cell state. Stem Cells 25:1231–1240. doi:10.1634/stemcells.2006-0617

Martin C, Chapman KE, Seckl JR, Ashley RH (1998) Partial cloning and differential expression of ryanodine receptor/calcium-release channel genes in human tissues including the hippocampus and cerebellum. Neuroscience 85:205–216. doi:10.1016/S0306-4522(97)00612-X

Martino G, Pluchino S (2006) The therapeutic potential of neural stem cells. Nat Rev Neurosci 7:395–406. doi:10.1038/nrn1908

Nakamura K, Ohya W, Funakoshi H, Sakaguchi G, Kato A, Takeda M, Kudo T, Nakamura T (2006) Possible role of scavenger receptor SRCL in the clearance of amyloid-β in Alzheimer's disease. J Neurosci Res 84:874–890. doi:10.1002/jnr.20992

Nakashima K, Takizawa T, Ochiai W, Yanagisawa M, Hisatsune T, Nakafuku M, Miyazono K, Kishimoto T, Kageyama R, Taga T (2001) BMP2-mediated alteration in the developmental pathway of fetal mouse brain cells from neurogenesis to astrocytogenesis. Proc Natl Acad Sci USA 98:5868–5873. doi:10.1073/pnas.101109698

Nishino J, Yamashita K, Hashiguchi H, Fujii H, Shimazaki T, Hamada H (2004) Meteorin: a secreted protein that regulates glial cell differentiation and promotes axonal extension. EMBO J 23:1998–2008. doi:10.1038/sj.emboj.7600202

Pallini R, Vitiani LR, Bez A, Casalbore P, Facchiano F, Di Giorgi Gerevini V, Falchetti ML, Fernandez E, Maira G, Peschle C, Parati E (2005) Homologous transplantation of neural stem cells to the injured spinal cord of mice. Neurosurgery 57:1014–1025. doi:10.1227/01.NEU.0000180058.58372.4c

Probst-Cousin S, Kowolik D, Kuchelmeister K, Kayser C, Neundörfer B, Heuss D (2002) Expression of annexin-1 in multiple sclerosis plaques. Neuropathol Appl Neurobiol 28:292–300. doi:10.1046/j.1365-2990.2002.00396.x

Prozorovski T, Schulze-Topphoff U, Glumm R, Baumgart J, Schröter F, Ninnemann O, Siegert E, Bendix I, Brüstle O, Nitsch R, Zipp F, Aktas O (2008) Sirt1 contributes critically to the redox-dependent fate of neural progenitors. Nat Cell Biol 10:385–394. doi:10.1038/ncb1700

Rabchevsky AG, Weinitz JM, Coulpier M, Fages C, Tinel M, Junier MP (1998) A role for transforming growth factor alpha as an inducer of astrogliosis. J Neurosci 18:10541–10552

Ruzinova MB, Benezra R (2003) Id proteins in development, cell cycle and cancer. Trends Cell Biol 13:410–418. doi:10.1016/S0962-8924(03)00147-8

Samanta J, Kessler JA (2004) Interactions between ID and OLIG proteins mediate the inhibitory effects of BMP4 on oligodendroglial differentiation. Development 131:4131–4412. doi:10.1242/dev.01273

Sato H, Ishida S, Toda K, Matsuda R, Hayashi Y, Shigetaka M, Fukuda M, Wakamatsu Y, Itai A (2005) New approaches to mechanism analysis for drug discovery using DNA microarray data combined with KeyMolnet. Curr Drug Discov Technol 2:89–98. doi:10.2174/1570163054064701

Satoh J, Tabunoki H, Nanri Y, Arima K, Yamamura T (2006) Human astrocytes express 14-3-3 sigma in response to oxidative and DNA-damaging stresses. Neurosci Res 56:61–72. doi:10.1016/j.neures.2006.05.007

Satoh J, Tabunoki H, Yamamura T, Arima K, Konno H (2007) TROY and LINGO-1 expression in astrocytes and macrophages/microglia in multiple sclerosis lesions. Neuropathol Appl Neurobiol 33:99–107. doi:10.1111/j.1365-2990.2006.00787.x

Schwab JM, Postler E, Nguyen TD, Mittelbronn M, Meyermann R, Schluesener HJ (2000) Connective tissue growth factor is expressed by a subset of reactive astrocytes in human cerebral infarction. Neuropathol Appl Neurobiol 26:434–440. doi:10.1046/j.1365-2990.2000.00271.x

Sergent-Tanguy S, Véziers J, Bonnamain V, Boudin H, Neveu I, Naveilhan P (2006) Cell surface antigens on rat neural progenitors and characterization of the CD3 (+)/CD3 (−) cell populations. Differentiation 74:530–541. doi:10.1111/j.1432-0436.2006.00098.x

Tatenhorst L, Senner V, Püttmann S, Paulus W (2004) Regulators of G-protein signaling 3 and 4 (RGS3, RGS4) are associated with glioma cell motility. J Neuropathol Exp Neurol 63:210–222

Taupin P, Ray J, Fischer WH, Suhr ST, Hakansson K, Grubb A, Gage FH (2000) FGF-2-responsive neural stem cell proliferation requires CCg, a novel autocrine/paracrine cofactor. Neuron 28:385–397. doi:10.1016/S0896-6273(00)00119-7

Tzeng SF, de Vellis J (1997) Expression and functional role of the Id HLH family in cultured astrocytes. Brain Res Mol Brain Res 46:136–142. doi:10.1016/S0169-328X(96)00294-X

Xu D, Hopf C, Reddy R, Cho RW, Guo L, Lanahan A, Petralia RS, Wenthold RJ, O'Brien RJ, Worley P (2003) Narp and NP1 form heterocomplexes that function in developmental and activity-dependent synaptic plasticity. Neuron 39:513–528. doi:10.1016/S0896-6273(03)00463-X

Yamagata K, Andreasson KI, Sugiura H, Maru E, Dominique M, Irie Y, Miki N, Hayashi Y, Yoshioka M, Kaneko K, Kato H, Worley PF (1999) Arcadlin is a neural activity-regulated cadherin involved in long term potentiation. J Biol Chem 274:19473–19479. doi:10.1074/jbc.274.27.19473

Yamanaka R, Arao T, Yajima N, Tsuchiya N, Homma J, Tanaka R, Sano M, Oide A, Sekijima M, Nishio K (2006) Identification of expressed genes characterizing long-term survival in malignant glioma patients. Oncogene 25:5994–6002. doi:10.1038/sj.onc.1209585

Yoshimatsu T, Kawaguchi D, Oishi K, Takeda K, Akira S, Masuyama N, Gotoh Y (2006) Non-cell-autonomous action of STAT3 in maintenance of neural precursor cells in the mouse neocortex. Development 133:2553–2563. doi:10.1242/dev.02419

Yu S, Zhang JZ, Xu Q (2006) Genes associated with neuronal differentiation of precursors from human brain. Neuroscience 141:817–825. doi:10.1016/j.neuroscience.2006.02.080

Disease Markers 27 (2009) 239–252
DOI 10.3233/DMA-2009-0670
IOS Press

Molecular network analysis suggests aberrant CREB-mediated gene regulation in the Alzheimer disease hippocampus

Jun-ichi Satoh[a,*], Hiroko Tabunoki[a] and Kunimasa Arima[b]
[a]*Department of Bioinformatics and Molecular Neuropathology, Meiji Pharmaceutical University, 2-522-1 Noshio, Kiyose, Tokyo 204-8588, Japan*
[b]*Department of Psychiatry, National Center Hospital, National Center of Neurology and Psychiatry, 4-1-1 Ogawahigashi, Kodaira, Tokyo 187-8551, Japan*

Abstract. The pathogenesis of Alzheimer disease (AD) involves the complex interaction between genetic and environmental factors affecting multiple cellular pathways. Recent advances in systems biology provide a system-level understanding of AD by elucidating the genome-wide molecular interactions. By using KeyMolnet, a bioinformatics tool for analyzing molecular interactions on the curated knowledgebase, we characterized molecular network of 2,883 all stages of AD-related genes (ADGs) and 559 incipient AD-related genes (IADGs) identified by global gene expression profiling of the hippocampal CA1 region of AD brains in terms of significant clinical and pathological correlations (Blalock et al., Proc Natl Acad Sci USA 101: 2173-2178, 2004). By the common upstream search, KeyMolnet identified cAMP-response element-binding protein (CREB) as the principal transcription factor exhibiting the most significant relevance to molecular networks of both ADGs and IADGs. The CREB-regulated transcriptional network included upregulated and downregulated sets of ADGs and IADGs, suggesting an involvement of generalized deregulation of the CREB signaling pathway in the pathophysiology of AD, beginning at the early stage of the disease. To verify the *in silico* observations *in vivo*, we conducted immunohistochemical studies of 11 AD and 13 age-matched control brains by using anti-phoshorylated CREB (pCREB) antibody. An abnormal accumulation of pCREB imunoreactivity was identified in granules of granulovacuolar degeneration (GVD) in the hippocampal neurons of AD brains. These observations suggest that aberrant CREB-mediated gene regulation serves as a molecular biomarker of AD-related pathological processes, and support the hypothesis that sequestration of pCREB in GVD granules is in part responsible for deregulation of CREB-mediated gene expression in AD hippocampus.

Keywords: Alzheimer disease, CREB, granulovacuolar degeneration, keymolnet, molecular network, systems biology

1. Introduction

Alzheimer disease (AD) is the most common cause of dementia worldwide, affecting the elderly population, characterized by the hallmark pathology of amyloid-β (Aβ) deposition and neurofibrillary tangle (NFT) formation in the brain. The complex interaction between genetic and environmental factors affecting multiple cellular pathways plays a role in the pathogenesis of AD [1]. The completion of the Human Genome Project in 2003 allows us to systematically characterize the comprehensive disease-associated profiles of the whole human genome. It promotes us to identify disease-specific and stage-specific molecular signatures and biomarkers for diagnosis and prediction of prognosis, and druggable targets for therapy [2]. Actually, global transcriptome analysis of AD brains identified a battery of genes aberrantly regulated in AD, whose role has not been previously

*Corresponding author: Prof. Dr. Jun-ichi Satoh, Department of Bioinformatics and Molecular Neuropathology, Meiji Pharmaceutical University, 2-522-1 Noshio, Kiyose, Tokyo 204-8588, Japan. Tel./Fax: +81 42 495 8678; E-mail: satoj@my-pharm.ac.jp.

ISSN 0278-0240/09/$17.00

predicted in its pathogenesis. They include reduced expression of kinases/phosphatases, cytoskeletal proteins, synaptic proteins, and neurotransmitter receptors in NFT-bearing CA1 neurons [3], downregulaton of neurotrophic factors and upregulation of proapoptotic molecules in the hippocampal CA1 region [4], disturbed sphingolipid metabolism in various brain regions during progression of AD [5], and overexpression of the AMPA receptor GluR2 subunit in synaptosomes of prefrontal cortex [6]. However, in global expression analysis, the important biological implications are often left behind to be characterized, because the huge amount of high-density microarray data is highly complex. Furthermore, cardinal observations obtained from *in silico* data analysis should be validated by independent wet lab experiments.

Recent advances in systems biology enable us to illustrate a cell-wide map of the complex molecular interactions with aid of the literature-based knowledgebase of molecular pathways [7,8]. In the scale-free molecular network, targeted disruption of several critical components, on which the biologically important molecular connections concentrate, could disturb the whole cellular function by destabilizing the network [9]. Thus, molecular network analysis goes beyond gene-by-gene analysis to shed light on a system-level understanding of molecular relationships among individual genes and networks.

The present study is designed to conduct molecular network analysis of a published microarray dataset of Blalock et al. [10]. It contains genome-wide expression profiling of hippocampal CA1 tissues derived from 22 AD patients with well-defined clinical and pathological stages. They identified 3,413 all stages of AD-related genes (ADGs) and 609 incipient AD-related genes (IADGs), and characterized overrepresented genes by using a bioinformatics tool named Expression Analysis Systematic Explorer (EASE). They found upregulation of tumor suppressors, oligodendrocyte growth factors, and protein kinase A (PKA) modulators, along with downregulation of protein folding/metabolism/transport machinery molecules in incipient AD (IAD) [10]. Recently, a different study followed up analysis of this dataset by weighted gene coexpression network analysis (WGCNA) that calculates a matrix containing all pairwise Pearson correlations between whole microarray probe sets across all subjects in an unsupervised manner. They identified AD-related coexpression modules that play key roles in synaptic transmission, extracellular transport, mitochondrial and metabolic functions, and myelination [11]. However, all of these studies did not clarify the common upstream transcription factors governing molecular networks, closely associated with deregulated gene expression in AD brains. By using KeyMolnet, a bioinformatics tool for analyzing molecular interactions on the curated knowledgebase [12], we characterized the most relevant molecular network of AD brain transcriptome, composed of the genes coordinately regulated by putative common upstream transcription factors.

2. Materials and methods

2.1. The dataset

We performed molecular network analysis of ADGs and IADGs, derived from a dataset of Blalock et al. [10]. It contains gene expression profiling of frozen tissues of the CA1 hippocampus, performed by analyzing with the Affymetrix Human Genome HG-U133A chip that contains 22,215 transcripts. The complete dataset is available from Gene Expression Omnibus (GEO) database (GSE1297). RNA was isolated from the samples of 31 age-matched individuals, composed of nine control subjects, seven patients with incipient AD (IAD), eight with moderate AD, and seven with severe AD [10]. The dataset was normalized following the Microarray Analysis Suite 5.0 (MAS5) algorithm. The clinical stage of AD was defined by the Mini-Mental State Examination (MMSE) score, i.e. control (MMSE $>$ 25), incipient AD (MMSE 20–26), moderate AD (MMSE 14–19), and severe AD (MMSE $<$ 14). The neurofibrillary tangle (NFT) burden was determined in each brain sample, which always showed an inverse relationship with the MMSE score. The statistical correlation between the expression levels of individual genes and the MMSE and NFT scores was evaluated by Pearson's correlation tests and ANOVA. With respect to overall correlations across 31 subjects, the study identified 3,413 ADGs, composed of 1,977 upregulated and 1,436 downregulated genes in all stages of AD patients versus control subjects. The study also identified 609 IADGs, composed of 431 upregulated and 178 downregulated genes in IAD patients versus control subjects.

2.2. Gene ID conversion

We converted Affymetrix probe IDs into the corresponding National Center for Biotechnology Information (NCBI) Entrez Gene IDs by using the

Database for Annotation, Visualization and Integrated Discovery (DAVID) 2008 Gene ID conversion tool (david.abcc.ncifcrf.gov) [13]. Then, we excluded a set of non-annotated genes, overlapping genes, and those listed concurrently in both upregulated and downregulated classes.

2.3. Molecular network analysis

KeyMolnet is a comprehensive knowledgebase, originally developed by the Institute of Medicinal Molecular Design (IMMD), Tokyo, Japan [12]. It covers virtually all the relationships heretofore reported among human genes, molecules, diseases, pathways and drugs, whose information is manually collected, carefully curated, and regularly updated by expert biologists. The database is categorized into the core contents collected from selected review articles with the highest reliability, or the secondary contents extracted from abstracts of PubMed database and Human Protein Reference database (HPRD). By importing microarray data, such as the list of Entrez Gene ID and fold changes of individual probes, KeyMolnet automatically provides corresponding molecules as a node on networks.

The common upstream search is a mode of network analysis that extracts the most relevant molecular network composed of the genes coordinately regulated by putative common upstream transcription factors. The generated network was compared side by side with 403 human canonical pathways of the KeyMolnet library. To reduce the potential bias toward the selection of major pathways, all well-established biological pathways covering both major and minor classes were collected by extensive search of valid review articles with journal impact factors greater than 10. Further information on the canonical pathways of KeyMolnet is available from IMMD upon request (www.immd.co.jp/en/keymolnet/index.html). The algorithm counting the number of overlapping molecular relations between the extracted network and the canonical pathway makes it possible to identify the canonical pathway showing the most significant contribution to the extracted network. It is constructed by modification of the algorithm developed for GO::TermFinder [14]. The significance in the similarity between the extracted network and the canonical pathway is scored following the formula, where O = the number of overlapping molecular relations between the extracted network and the canonical pathway, V = the number of molecular relations located in the extracted network, C = the number of molecular relations located in the canonical pathway, T = the number of total molecular relations composed of approximately 110,000 sets, and the X = the sigma variable that defines coincidence.

$$\text{Score} = -\log_2(\text{Score}(p))$$

$$\text{Score}(p) = \sum_{x=O}^{Min(C,V)} f(x)$$

$$f(x) = {}_C C_x \cdot {}_{T-C} C_{V-x} / {}_T C_V$$

2.4. Immunohistochemistry

The autopsied brain samples were provided by Research Resource Network (RRN), Japan. Written informed consent was obtained form all the cases. The Ethics Committee of National Center of Neurology and Psychiatry approved the present study. The study population consists of 11 AD patients composed of five men and six women with the mean age of 71 ± 9 years, and 13 other neurological disease (termed as non-AD) patients composed of six men and seven women with the mean age of 69 ± 9 years. The non-AD cases include three patients with Parkinson disease (PD), two with multiple system atrophy (MSA), four with amyotrophic lateral sclerosis (ALS), and four with myotonic dystrophy. The average of brain weight was 1,038 ± 163 gram in AD cases and 1,195 ± 182 gram in non-AD cases. Brain tissues of the hippocampus and the motor cortex were fixed with 4% paraformaldehyde (PFA), embedded in paraffin, and processed for ten micron-thick serial sections. All AD cases were satisfied with the Consortium to Establish a Registry for Alzheimer's Disease (CERAD) criteria for diagnosis of definite AD [15]. They were categorized into the stage C of amyloid deposition and the stage VI of neurofibrillary degeneration, following the Braak's staging [16].

The immunohistochemistry protocol was described elsewhere [17]. In brief, after deparaffination, tissue sections were heated in 10 mM citrate sodium buffer, pH 6.0 by autoclave at 125°C for 30 sec in a temperature-controlled pressure chamber (Dako, Tokyo, Japan). They were incubated with 3% hydrogen peroxide-containing methanol to block the endogenous peroxidase activity, and with phosphate-buffered saline (PBS) containing 10% normal goat serum (NGS) at room temperature (RT) for 15 min to block non-specific staining. Then, tissue sections were stained at 4°C overnight with rabbit polyclonal anti-phoshorylated cAMP-response element-binding protein (pCREB) an-

tibody at a dilution of 1:1,000 (Y011052; Applied Biological Materials, Richmond, BC, Canada). This antibody was produced against a synthesized phosphopeptide spanning R-P-SP-Y-R, derived from the human CREB1 amino acid sequences surrounding the serine 133 residue (Ser-133), and purified by affinity-chromatography with an epitope-specific phosphopeptide. The specificity of the antibody was verified by western blot analysis of a human neuronal cell line exposed to forskolin in culture (not shown). After several washes, the tissue sections were incubated with horseradish peroxidase (HRP)-conjugated anti-rabbit antibody (Nichirei, Tokyo, Japan), and colorized with DAB substrate (Vector Laboratories, Burlingame, CA, USA), followed by a counterstain with hematoxylin. The adjacent sections were immunolabeled with mouse monoclonal anti-GFAP antibody (Nichirei). For negative controls, the step of incubation with primary antibodies was omitted.

3. Results

3.1. *Transcriptome dataset of Alzheimer disease hippocampus*

The dataset of Blalock et al. [10] contains genome-wide transcriptome of the hippocampus CA1 region, derived from nine control subjects, seven patients with incipient AD (IAD), eight with moderate AD, and seven with severe AD. They identified 3,413 all stages of AD-related genes (ADGs) and 609 IAD-related genes (IADGs) based on significant clinical and pathological correlations. We performed extensive curation of their data, and extracted 2,883 Entrez Gene IDs of ADGs, composed of 1,675 upregulated and 1,208 downregulated genes in all stages of AD patients versus control subjects (Supplementary Tables 1 and 2 online). We also identified 559 Entrez Gene IDs of IADGs, composed of 395 upregulated and 164 downregulated genes in IAD patients versus control subjects (Supplementary Tables 3 and 4 online).

3.2. *The molecular network analysis of ADGs and IADGs identified CREB as a central transcription factor*

First, we imported 2,883 Entrez Gene IDs of ADGs, along with the expression levels, into KeyMolnet (the version 4.9.9.616 of July 1, 2009). The common upstream search of the core contents generated a complex network composed of 508 fundamental nodes with 735 molecular relations, arranged with respect to subcellular location of the molecules by the editing function of KeyMolnet (Fig. 1). By statistical evaluation, the extracted network showed the most significant relationship with transcriptional regulation by CREB with the score of 229 and score (p) = 1.141E-069, where CREB is located as a common upstream transcription factor that has direct connections with 50 nodes, all of which are known CRE-responsive genes (Fig. 2 and Table 1). Unexpectedly, the CREB-regulated transcriptional network is comprised of not only 17 upregulated ADGs but also 26 downregulated ADGs. These results suggest not simply either overactivation or hypoactivation of CREB but an involvement of generalized deregulation of the CREB signaling pathway in the pathophysiology of AD. The second rank pathway was transcriptional regulation by nuclear factor kappa B (NF-κB) with the score of 158 and score (p) = 1.945E-048 (Supplementary Fig. 1 online), while the third rank was transcriptional regulation by vitamin D receptor (VDR) with the score of 140 and score (p) = 5.841E-042 (Supplementary Fig. 2 online).

Next, we imported 559 Entrez Gene IDs of IADGs and the expression levels into KeyMolnet. Subsequently, the common upstream search of the core contents generated a less complex network composed of 143 fundamental nodes with 190 molecular relations (Fig. 3). By statistical evaluation, the extracted network showed again the most significant relationship with transcriptional regulation by CREB with the score of 71 and score (p) = 3.325E-022, comprised of 5 upregulated and 5 downregulated IADGs (Fig. 4 and Table 1). These results suggest that functional impairment of CREB in the AD hippocampus is beginning at the early stage of the disease. The second rank pathway was transcriptional regulation by NF-κB or by glucocorticoid receptor (GR) with the identical score of 53 and score (p) = 1.163E-016 between both.

3.3. *Granulovacuolar degeneration in hippocampal neurons of AD brains expressed pCREB immunoreactivity*

It is well known that a wide range of extracellular stimuli activates CREB by inducing phosphorylation of Ser-133 on CREB, thereby it functions as a transcriptional activator [18,19]. Because the molecular network of both ADGs and IADGs reflects persistent impairment of CREB function in the AD hippocampus, we studied the expression of Ser-133-phosphorylated

Table 1
The list of 51 genes constructing the CREB-regulated transcriptional network in AD hippocampus

KeyMolnet symbol	Gene name	Upregulation or downregulation[a]	Involvement in IAD network	Swiss-Prot ID
14-3-3epsilon	14-3-3 protein epsilon	down		P62258
AChE	acetylcholinestrase	down		P22303
AhR	arylhydrocarbon receptor	km		P35869
BCKDH	branched-chain alpha-keto acid dehydrogenase	down		P09622, P11182, P12694, P21953
Bcl-2	B-cell lymphoma 2	up		P10415
BiP	78 kDa glucose-regulated protein	down	yes	P11021
BRCA1	breast cancer type 1 susceptibility protein	up		P38398
C/EBPb	CCAAT/enhancer binding protein beta	km	yes	P17676
CCK	cholecystokinin	down		P06307
CDK5	cyclin dependent kinase 5	down		Q00535
ChromograninA	chromogranin A	down		P10645
CPT	carnitine palmitoyl transferase	up	yes	P50416, Q92523, Q8TCG5, P23786
CREB	cAMP-response-element-binding-protein	km	yes	P16220
CRF	corticotropin-releasing factor	down	yes	P06850
cyclinA	cyclin A	down		P78396, P20248
cyto-c	cytochrome c	down		P99999
DIO2	type II iodothyronine deiodinase	down		Q92813
Egr1	early growth response protein 1	up		P18146
ENO2	neuron-specific enolase	down		P09104
FN1	fibronectin 1	down		P02751
GADD34	protein phosphatase 1, regulatory subunit 15A	up		O75807
GluR1	glutamate receptor 1	down		P42261
GR	glucocorticoid receptor	km	yes	P04150
GS	glutamine synthetase	down	yes	P15104
HO-1	heme oxygenase 1	up		P09601
ICAM-1	intercellular adhesion molecule 1	up		P05362
IGF1	insulin-like growth factor 1	down		P01343, P05019
IL-6	interleukin-6	up		P05231
JunD	transcription factor Jun-D	up	yes	P17535
LDH	L-lactate dehydrogenase	down		Q6ZMR3, Q9BYZ2, P00338, P07195, P07864
MITF	microphthalmia-associated transcription factor	up	yes	O75030
MnSOD	manganese superoxide dismutase	up		P04179
NF-L	neurofilament triplet L protein	down		P07196
NPY	neuropeptide Y	down		P01303
NR4A2	orphan nuclear receptor NR4A2	km		P43354
ODC	ornithine decarboxylase	up		P11926
PC	prohormone convertase	down		P29120, P16519, Q16549
PCB	pyruvate carboxylase	up	yes	P11498
PCNA	proliferating cell nuclear antigen	down		P12004
PER1	period circadian protein 1	up	yes	O15534
PER2	period circadian protein 2	up		O15055
Pit-1	pituitary-specific positive transcription factor 1	km	yes	P28069
PPT-A	preprotachykinin A	down	yes	P20366
proenkeph	proenkephalin	down		P01213, P01210
SGK	serum- and glucocorticoid-inducible kinase	up	yes	O00141, Q9HBY8, Q96BR1
SST	somatostatin	down	yes	P61278
STAT3	signal transducer and activator of transcription 3	km	yes	P40763
SynapsinI	synapsin-1	down		P17600
TGFb2	transforming growth factor beta 2	up		P61812
TyrAT	tyrosine aminotransferase	up		P17735
VIP	vasoactive intestinal peptide	down		P01282

Km represents additional nodes unlisted in the original set of 2,883 ADGs but automatically incorporated from KeyMolnet core contents following the network-searching algorithm.

CREB (pCREB) in 11 AD and 13 age-matched control brains by immunohistochemistry. The granular components of granulovacuolar degeneration (GVD), accumulated in the cytoplasm of hippocampal pyramidal neurons in both AD and non-AD brains, expressed strong immunoreactivity against pCREB (Fig. 5, panels a-d). However, the nuclei of hippocampal pyramidal neurons were devoid of pCREB immunoreac-

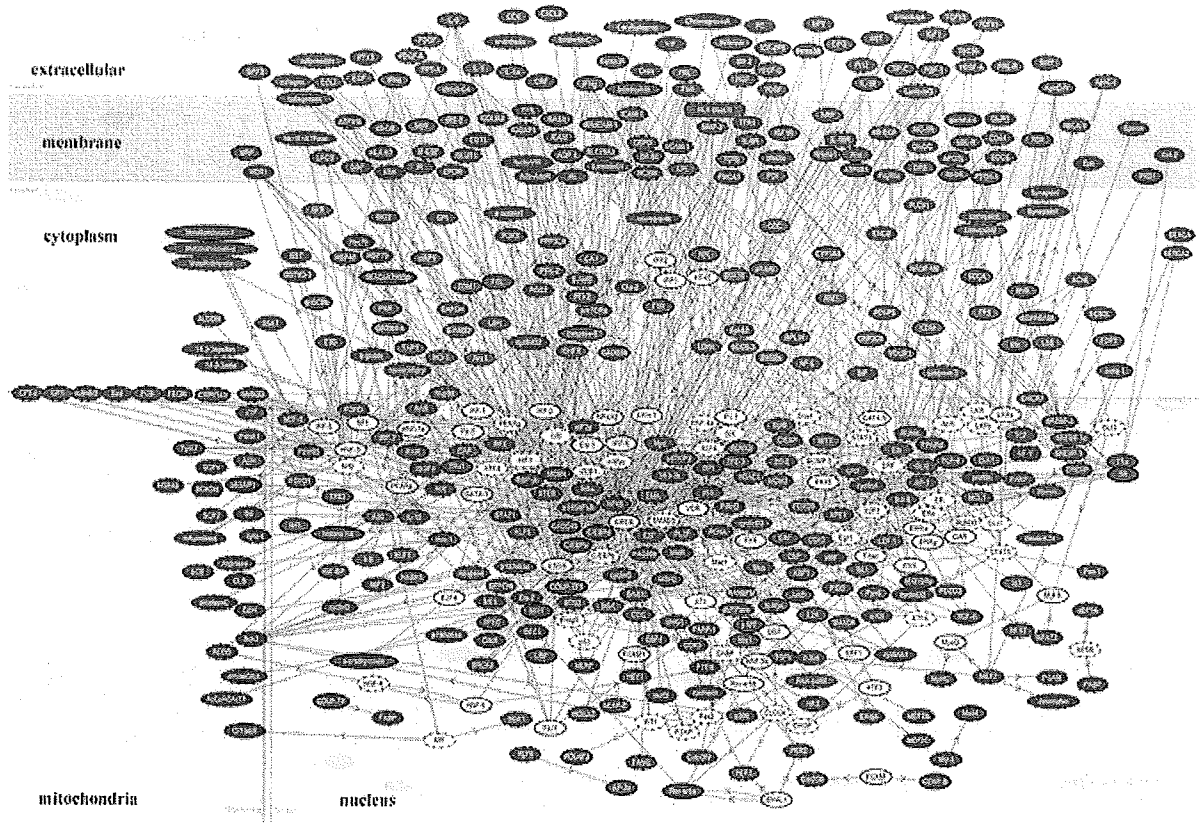

Fig. 1. Molecular network of all stages of AD-related genes (ADGs). The list of 2,883 Entrez Gene IDs corresponding to ADGs was imported into KeyMolnet. The common upstream search of the core contents generated a network composed of 508 fundamental nodes with 735 molecular relations, arranged with respect to subcellular location of the molecules. Red nodes represent upregulated genes, whereas blue nodes represent downregulated genes. White nodes exhibit additional nodes extracted automatically from the core contents incorporated in the network to establish molecular connections. The direction of molecular relation is indicated by red-colored dash line with arrow (transcriptional activation) or blue-colored dash line with arrow and stop (transcriptional repression).

tivity. In addition, the vacuolar component of GVD lacked pCREB immunoreactivity, while neuritic processes of hippocampal neurons expressed variable levels of pCREB immunoreactivity (Fig. 5, panel c). pCREB-immunoreactive GVD-bearing neurons were distributed chiefly in the CA1-CA3 sectors. Senile plaques and neurofibrillary tangles were completely devoid of pCREB immunolabeling. Although the number of pCREB-immunoreactive GVD-bearing neurons was varied among the cases, it was significantly greater in the hippocampus of AD compared with non-AD ($p = 0.00020$ by Mann-Whiteney's U test) (Fig. 6). pCREB-immunoreactive GVD-bearing neurons were occasionally found in the CA4 and subicular regions of AD brains, but barely detectable in the corresponding regions of non-AD brains. In both AD and non-AD brains, substantial numbers of neuronal axons distributed in the white matter of the motor cortex expressed intense pCREB immunoreactivity (Fig. 5, panel e). In both AD and non-AD brains, a subpopulation of reactive astrocytes and almost all ependymal cells expressed strong pCREB immunoreactivity, but it was located predominantly in their nuclei (Fig. 5, panel f). In both AD and non-AD brains, most neurons except for hippocampal pyramidal neurons did not express discernible pCREB immunoreactivity in their cell bodies and nuclei. Neither oligodendrocytes nor microglia expressed pCREB immunoreactivity in any cases examined.

4. Discussion

Since microarray analysis usually produces a large amount of gene expression data at one time, it is often difficult to find out the meaningful relationship be-

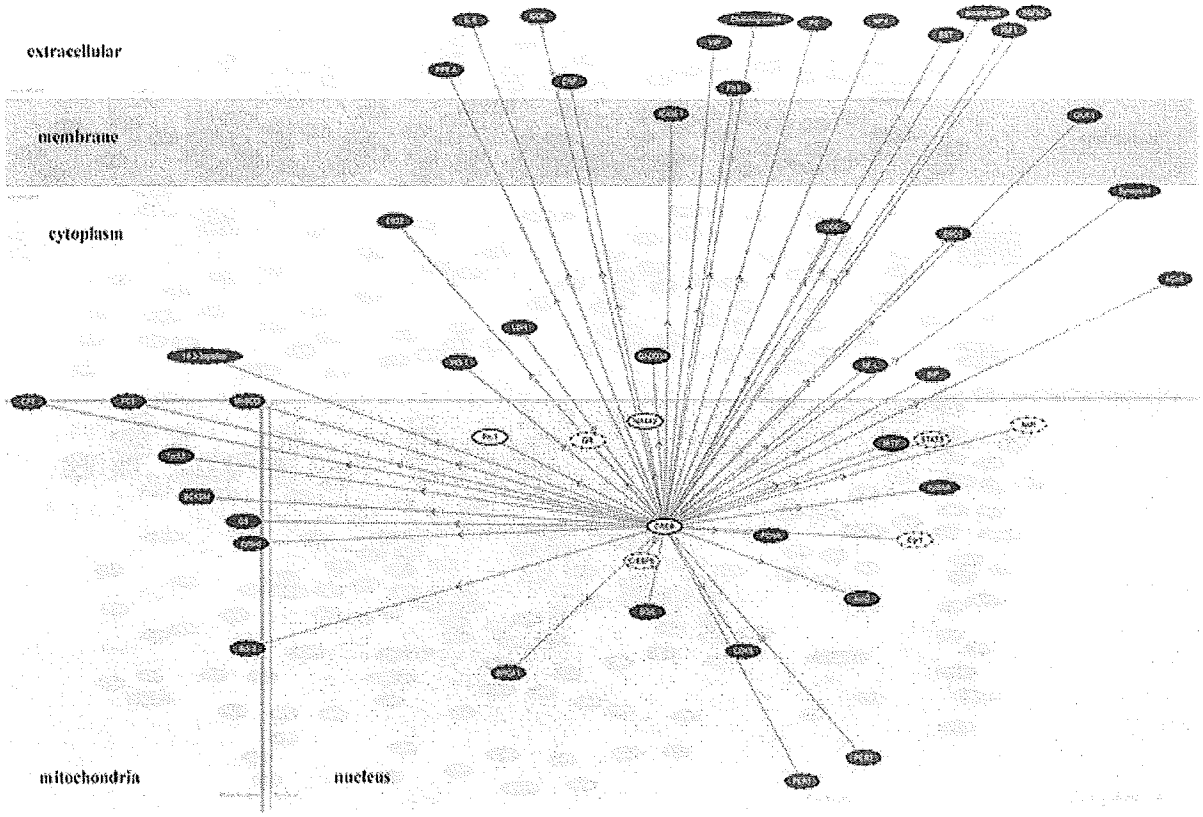

Fig. 2. The CREB-regulated transcriptional network of ADGs. The CREB-regulated transcriptional network extracted from the ADG network of Fig. 1 consists of a central node of CREB and 50 connecting nodes of CREB target genes listed in Table 1.

tween gene expression profile and biological implications from such a large quantity of available data. To overcome this difficulty, we have made a breakthrough to identify the molecular network most closely associated with microarray data by using a novel bioinformatics tool named KeyMolnet [12]. KeyMolnet includes the highly reliable information on a wide range of human proteins, small molecules, molecular relations, diseases, and drugs. All the contents are manually collected and carefully curated by experts from the literature and public databases. The application of KeyMolnet has an advantage that the user can easily merge microarray data with the comprehensive knowledgebase to characterize pathophysiologically meaningful networks from the high-throughput gene expression data [20,21]. In particular, the common upstream search is the most powerful approach to identify a battery of common transcription factors governing molecular networks closely associated with aberrant gene expression. By using KeyMolnet, we characterized the molecular network of 2,883 ADGs and 559 IADGs that show significant correlations with MMSE score and NFT burden in either all stages of AD or the early stage of AD [10]. We identified CREB as the central transcription factor that exhibits the most significant relevance to molecular networks of both ADGs and IADGs.

CREB is the prototype stimulus-inducible transcription factor binding as a dimer to a conserved cAMP-responsive element (CRE) of the target genes [18,19]. CREB is promptly activated in response to a wide range of extracellular stimuli, such as growth factors, peptide hormones, and neuronal activity, all of which activate various protein kinases such as PKA, mitogen-activated protein kinases (MAPKs), and Ca^{2+}/calmodulin-dependent protein kinases (CAMKs). They phosphorylate Ser-133 located in the KID domain of CREB. The phosphorylation of Ser-133 on CREB (pCREB) induces the recruitment of a transcriptional coactivator named CREB binding protein (CBP), thereby activates the expression of CRE-responsive genes. The CREB target genes play key roles in neuronal devel-

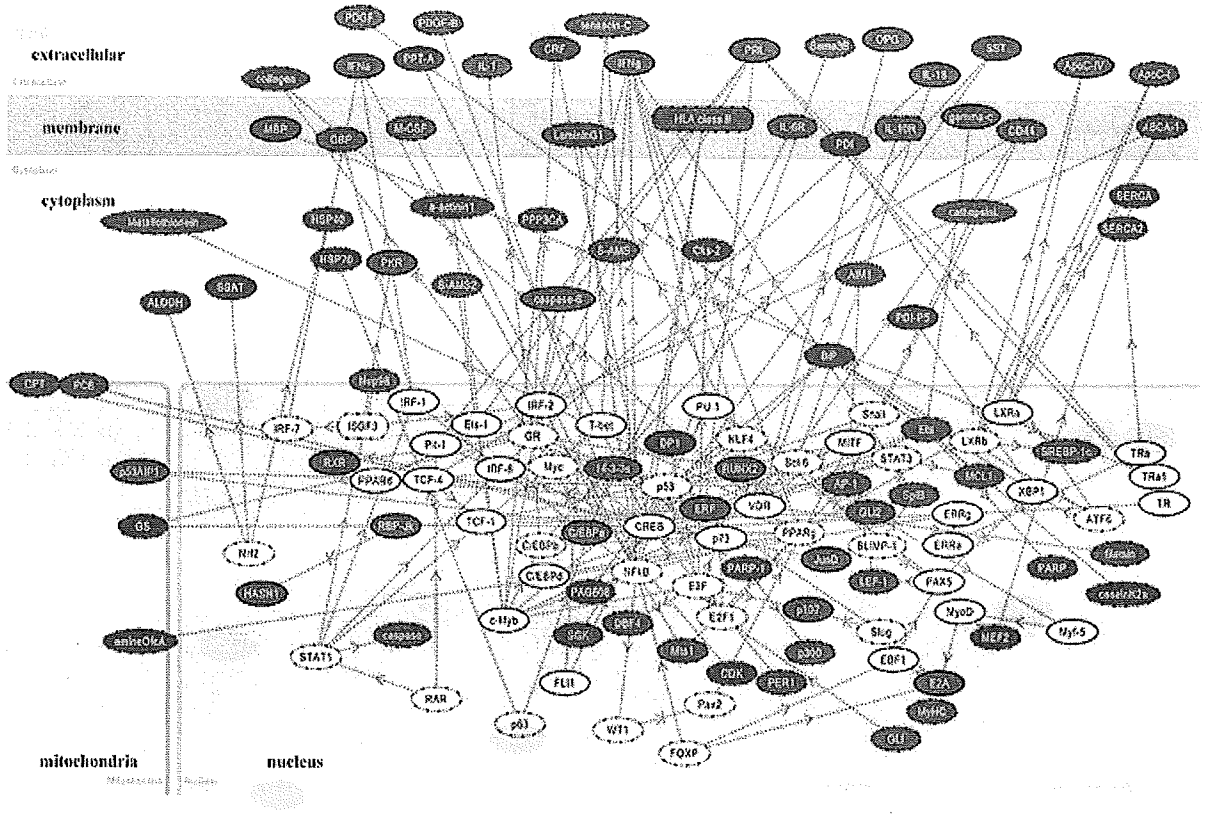

Fig. 3. Molecular network of incipient AD-related genes (IADGs). The list of 559 Entrez Gene IDs corresponding to IADGs was imported into KeyMolnet. The common upstream search of the core contents generated a network composed of 143 fundamental nodes with 190 molecular relations, arranged with respect to subcellular location of the molecules. Red nodes represent upregulated genes, whereas blue nodes represent downregulated genes. White nodes exhibit additional nodes extracted automatically from the core contents incorporated in the network to establish molecular connections. The direction of molecular relation is indicated by red-colored dash line with arrow (transcriptional activation) or blue-colored dash line with arrow and stop (transcriptional repression).

opment, synaptic plasticity, and neuroprotection in the central nervous system (CNS). Currently, we are able to search thousands of CREB target genes via the web-accessible database (natural.salk.edu/CREB) [22]. In the present study, the CREB-regulated transcriptional network consisted of both upregulated and downregulated sets of ADGs and IADGs. These observations suggest not simply either overactivation or hypoactivation of CREB but an involvement of generalized deregulation of the CREB signaling pathway in the pathophysiology of AD, emerging at the early stage of the disease.

To verify the *in silico* observations *in vivo*, we conducted immunohistochemical studies of 11 AD and 13 age-matched non-AD control brains by using anti-pCREB antibody. We identified aberrant pCREB immunoreactivity concentrated in granules of GVD in the hippocampus of both AD and non-AD brains, where the number of pCREB-immunoreactive GVD-bearing neurons was significantly greater in AD than non-AD cases. These results suggest that pCREB-immunoreactive GVD does not itself serve as an AD-specific diagnostic marker. However, these observations would support the hypothesis that sequestration of pCREB in GVD granules might be in part attributable to disturbed CREB-regulated gene expression in AD hippocampus.

Physiologically, CREB plays a pivotal role in the long-term memory formation in CA1 hippocampal neurons [23]. A previous study by western blot analysis showed that pCREB levels are reduced in AD brain tissues, although the cellular and subcellular location of pCREB was not characterized [24]. In a rat model, cortical impact injury induces a cognitive impairment, associated with reduced expression of CREB and target genes in the ipsilateral hippocampus [25]. A phosphodiesterase-4 inhibitor rolipram, by activating the cAMP/PKA/CREB signaling pathway, ameliorates deficits in long-term potential and cognitive function

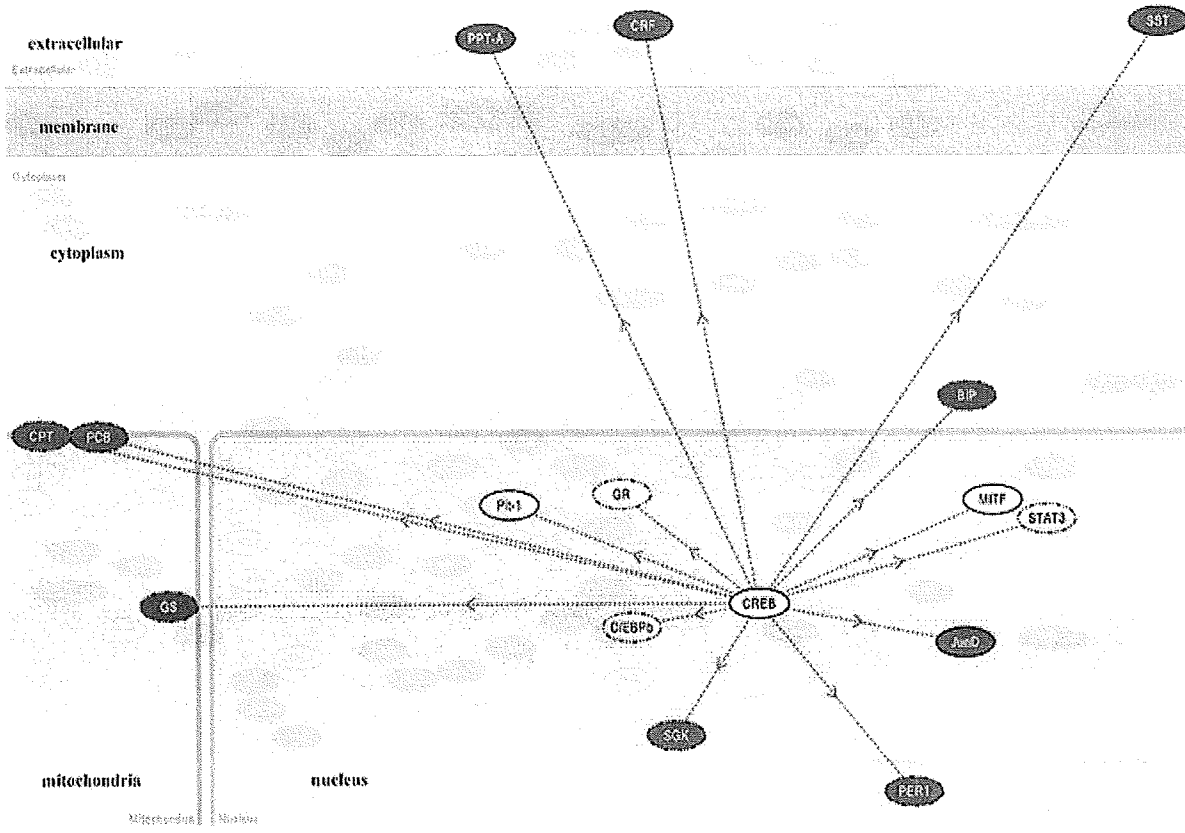

Fig. 4. The CREB-regulated transcriptional network of IADGs. The CREB-regulated transcriptional network extracted from the IADG network of Fig. 3 consists of a central node of CREB and 15 connecting nodes of CREB target genes listed in Table 1.

in a transgenic mouse model of AD [26]. Overactivation of calpain induces proteolysis of PKA subunits, resulting in inactivation of CREB in AD brains [27]. High levels of intracellular Aβ induce sustained hyperphosphorylation of CREB that blocks nuclear translocation of pCREB, resulting in inactivation of CREB-regulated gene expression [28]. The Aβ oligomers inactivate MAPKs, PKA, and cyclic GMP-dependent protein kinase essential for CREB activation in hippocampal neurons [29–31]. Long-term treatment with green tea catechin reduces the levels of Aβ oligomers, thereby restores the expression of CREB target genes, such as BDNF and PSD95, in the hippocampus [32]. All of these observations support a possible scenario that a defect in the CREB-mediated signaling pathway in hippocampal neurons causes cognitive disturbance during progression of AD. Therefore, CREB serves as a promising molecular target for treatment of dementia in AD [33].

The accumulation of misfolded cellular proteins within neurons, due to a defect in the clearance system, such as the ubiquitin-proteasome system (UPS) and the autophagic-lysosomal system, is a pathological hallmark of various neurodegenerative diseases [34]. Degradation of CREB involves nuclear export of CREB, modification by polyubiquitination, and processing for proteasomes, suggesting that UPS is a major system for CREB degradation under normal physiological conditions [35,36]. We identified an abnormal accumulation of pCREB in GVD granules of hippocampal neurons in AD brains. GVD is a pathological change characterized by electron-dense granules within double membrane-bound cytoplasmic vacuoles that highly resemble autophagosomes [37]. The emergence of GVD is confined to hippocampal pyramidal neurons of AD brains, and infrequently found in those of other neurodegenerative diseases. GVD is barely detectable in other brain regions. It plays a role in sequestration and degradation of unnecessary proteins and organelles in neurons exposed to aging-related stressful insults [37]. The active forms of caspase-3, glycogen synthase kinase-3β (GSK-3β), c-Jun N-terminal kinase

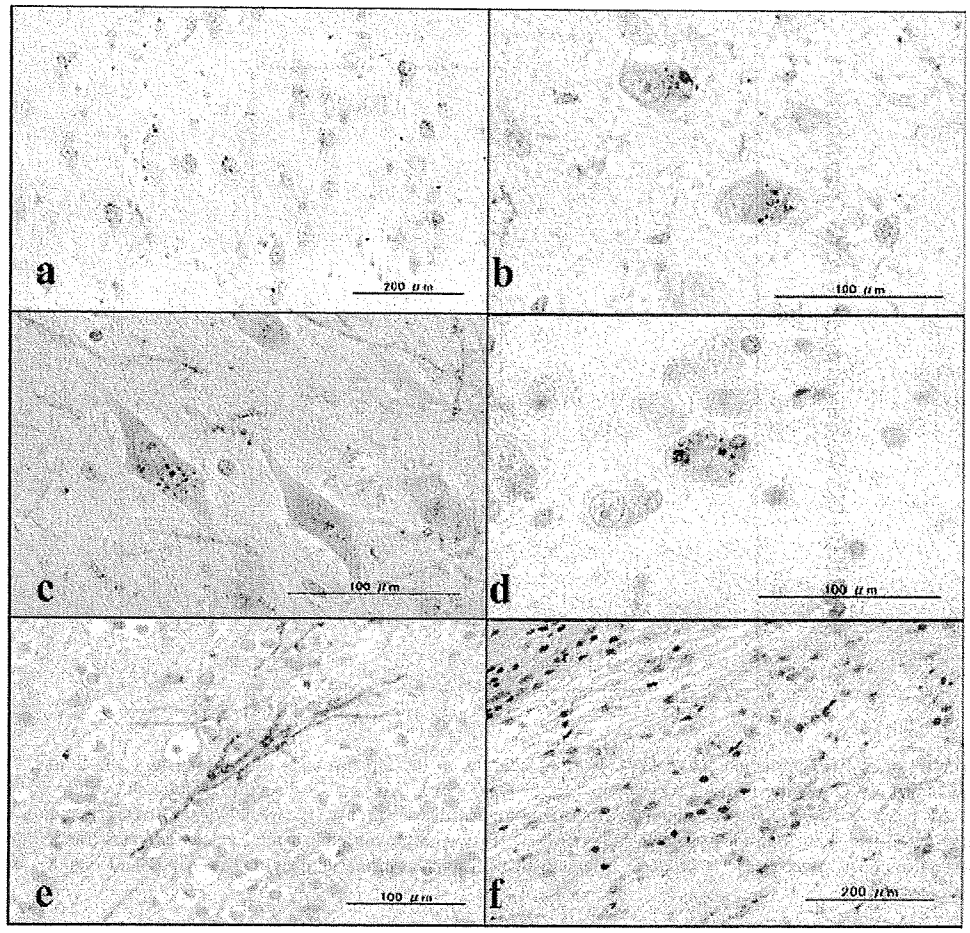

Fig. 5. pCREB immunoreactivity in AD and non-AD brains. The tissue sections of the hippocampus (HC) and the motor cortex (MC) of 11 AD patients and 13 other neurological disease (non-AD) patients were immunolabeled with an antibody against Ser-133-phosphorylated CREB (pCREB). (a) HC CA1 of a 59-year-old AD patient. The granular components of granulovacuolar degeneration (GVD) accumulated in the cytoplasm of pyramidal neurons exhibit strong pCREB immunoreactivity. (b) HC CA1 of a 68-year-old AD patient. The granular components of GVD accumulated in the cytoplasm of pyramidal neurons exhibit strong pCREB immunoreactivity. (c) HC CA3 of a 77 year-old AD patient. The vacuolar components of GVD are devoid of pCREB immunoreactivity. Neuritic processes of hippocampal neurons express variable levels of pCREB immunoreactivity. (d) HC CA1 of a 68 year-old myotonic dystrophy patient. The granular components of GVD accumulated in the cytoplasm of pyramidal neurons exhibit strong pCREB immunoreactivity. (e) MC of a 72-year-old AD patient. Substantial numbers of neuronal axons in the white matter of the motor cortex express strong pCREB immunoreactivity. (f) The periventricular white matter in the hippocampus of an 80 year-old AD patient. A subpopulation of reactive astrocytes express strong pCREB immunoreactivity located predominantly in their nuclei.

(JNK), c-Jun, pancreatic eIF2-alpha kinase (PERK), and TAR DNA-binding protein-43 (TDP-43), all of which are modified by phosphorylation, are found to be accumulated in GVD granules of hippocampal neurons in AD brains [38–43]. GVD granules also include cytoskeletal proteins, such as neurofilament, tubulin, and tau, along with ubiquitin [44,45]. At present, the precise implication of pCREB accumulation in GVD granules of hippocampal neurons in AD brains remains unknown. Importantly, degenerating neurons but not apparently healthy neurons in AD brains exhibit the profuse accumulation of autophagic vacuoles (AVs), owing to decreased clearance of AVs [46], suggesting an involvement of impaired autophagy function in formation of pCREB-accumulated GVD granules.

We found that neuronal axons, neuritic processes, and a subpopulation of reactive astrocytes also express pCREB immunoreactivity in both AD and non-AD brains. In a rat model of neuronal injury, reactive astrocytes express pCREB following intracerebroventricular injection of kinate [47]. In developing mouse DRG neurons, CREB protein is translated in response to NGF from the corresponding mRNA located in axons, and subsequently translocated to the cell body via a retro-

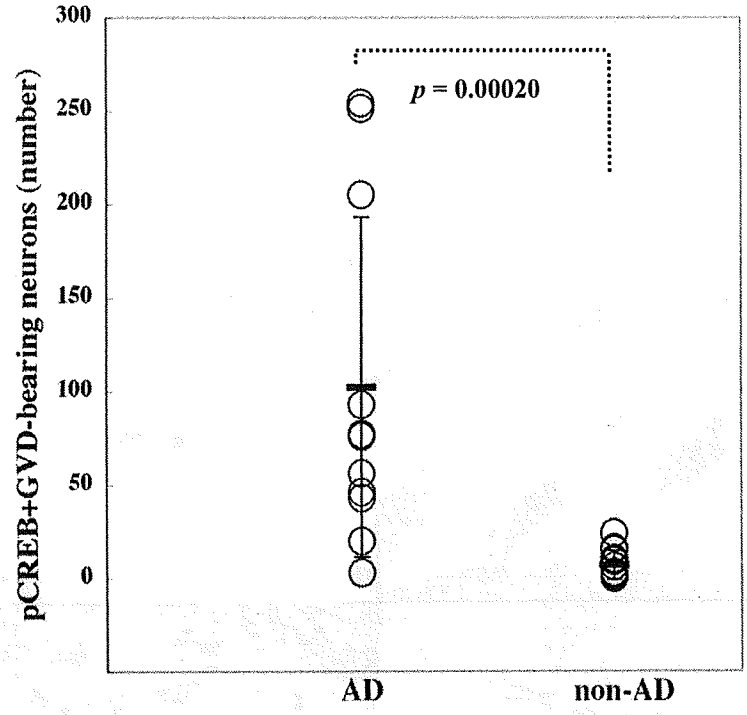

Fig. 6. The number of pCREB-immunoreactive GVD-bearing neurons in the hippocampus of AD and non-AD brains. The number of pCREB-immunoreactive GVD-bearing neurons was counted in the CA1, CA2, CA3 and CA4 sectors and the subiculum of the hippocampus, derived from 11 AD cases and 13 age and sex-matched other neurological disease (non-AD) cases. Non-AD cases include three patients with Parkinson disease (PD), two with multiple system atrophy (MSA), four with amyotrophic lateral sclerosis (ALS), and four with myotonic dystrophy. The total number in each case is plotted. The statistical difference in the numbers between AD and non-AD was evaluated by Mann-Whitney's U test.

grade axonal transport [48]. These observations would provide an explanation for glial or axonal location of CREB and pCREB.

We identified NF-κB-regulated gene expression as the second significant pathway in the molecular network of AGDs and IADGs (Supplementary Fig. 1 online). The NF-κB family, consisting of NF-κB1 (p50/p105), NF-κB2 (p52/p100), RelA (p65), RelB, and c-Rel, acts as a central regulator of innate and adaptive immune responses, cell proliferation, and apoptosis [49]. Under unstimulated conditions, NF-κB is sequestrated in the cytoplasm via non-covalent interaction with the inhibitor of NF-κB (IκB). Proinflammatory cytokines and stress-inducing agents activate specific IκB kinases that phosphorylate IκB proteins. Phosphorylated IκBs are ubiquitinated, and then processed for proteasome-mediated degradation, resulting in nuclear translocation of NF-κB that regulates the expression of hundreds of target genes by binding to the consensus sequence located in the promoter. Importantly, the expression of NF-κB p65 is enhanced in neurons, NFTs, and dystrophic neurites in the hippocampus and entorhinal cortex of AD brains [50]. A NF-κB-inducible microRNA, MiR-146a, reduces the expression of complement factor H (CFH), a negative regulator of proinflammatory responses in AD brains [51].

We also identified gene expression regulated by vitamin D receptor (VDR) as the third significant pathway in the molecular network of AGDs (Supplementary Fig. 2 online). Vitamin D plays a neuroprotective role by modulating neuronal calcium homeostasis. By forming a heterodimer with the retinoid X receptor (RXR), VDR activates the transcription of target genes with the vitamin D response element (VDRE) in the promoter. A significant association is found between VDR gene polymorphism and development of AD [52]. In AD brains, the expression of VDR and its target calbindin D28K is downregulated in hippocampal CA1 neurons [53].

In conclusion, KeyMolnet has effectively characterized molecular network of 2,883 ADGs and 559 IADGs. The common upstream search identified CREB as the principal transcription factor that regulates molecular networks of both ADGs and IADGs. Im-